nature COMMUNICATIONS

ARTICLE

Received 16 Jul 2014 | Accepted 12 Dec 2014 | Published 30 Jan 2015

DOI: 10.1038/ncomms7137 OPEN

Augmented AMPK activity inhibits cell migration by phosphorylating the novel substrate Pdlim5

Yi Yan[1,*], Osamu Tsukamoto[1,*], Atsushi Nakano[2], Hisakazu Kato[1], Hidetaka Kioka[3], Noriaki Ito[3], Shuichiro Higo[3], Satoru Yamazaki[4], Yasunori Shintani[1], Ken Matsuoka[3], Yulin Liao[5], Hiroshi Asanuma[2], Masanori Asakura[2], Kazuaki Takafuji[6], Tetsuo Minamino[3], Yoshihiro Asano[3], Masafumi Kitakaze[2] & Seiji Takashima[1,7]

Augmented AMP-activated protein kinase (AMPK) activity inhibits cell migration, possibly contributing to the clinical benefits of chemical AMPK activators in preventing atherosclerosis, vascular remodelling and cancer metastasis. However, the underlying mechanisms remain largely unknown. Here we identify PDZ and LIM domain 5 (Pdlim5) as a novel AMPK substrate and show that it plays a critical role in the inhibition of cell migration. AMPK directly phosphorylates Pdlim5 at Ser177. Exogenous expression of phosphomimetic S177D-Pdlim5 inhibits cell migration and attenuates lamellipodia formation. Consistent with this observation, S177D-Pdlim5 suppresses Rac1 activity at the cell periphery and displaces the Arp2/3 complex from the leading edge. Notably, S177D-Pdlim5, but not WT-Pdlim5, attenuates the association with Rac1-specific guanine nucleotide exchange factors at the cell periphery. Taken together, our findings indicate that phosphorylation of Pdlim5 on Ser177 by AMPK mediates inhibition of cell migration by suppressing the Rac1-Arp2/3 signalling pathway.

[1] Department of Medical Biochemistry, Osaka University Graduate School of Medicine, 2-2 Yamadaoka, Suita, Osaka 565-0871, Japan. [2] Department of Clinical Research and Development, National Cerebral and Cardiovascular Center Research Institute, Suita, Osaka 565-8565, Japan. [3] Department of Cardiovascular Medicine, Osaka University Graduate School of Medicine, 2-2 Yamadaoka, Suita, Osaka 565-0871, Japan. [4] Department of Cell Biology, National Cerebral and Cardiovascular Center Research Institute, Suita, Osaka 565-8565, Japan. [5] Department of Cardiology, Nanfang Hospital, Southern Medical University, 1838 North Guangzhou Avenue, 510515 Guangzhou, China. [6] Center for Research Education, Osaka University Graduate School of Medicine, 2-2 Yamadaoka, Suita, Osaka 565-0871, Japan. [7] Japan Science and Technology Agency-Core Research for Evolutional Science and Technology (CREST), Kawaguchi 332-0012, Japan. * These authors contributed equally to this work.. Correspondence and requests for materials should be addressed to O.T. (email: tsuka@medbio.med.osaka-u.ac.jp).

© 2015 Macmillan Publishers Limited. All rights reserved.

AMP-activated protein kinase (AMPK), generally considered an energy sensor kinase, requires AMP for activation[1]. Recently, a growing body of evidence has revealed that AMPK also plays a key role in the establishment of cell polarity and motility[2,3]. We previously reported that AMPK regulates cell migration by controlling microtubule dynamics through phosphorylation of a cytoplasmic linker protein-170 (CLIP-170)[4]. Moreover, recent studies have implicated AMPK in the regulation of actin cytoskeleton dynamics and reorganization at the plasma membrane[5,6]. Thus, AMPK is predicted to regulate cell migration by controlling both microtubule and actin-filament dynamics.

Cell migration is a physically integrated molecular process that begins with dynamic polarization and formation of lamellipodia, membrane protrusions at the leading edges of cells[7]. Rac1, a Rho-family small GTPase, is a key upstream regulator of actin dynamics and organization, and is necessary for the formation of persistent lamellipodia leading to directional cell migration[8,9]. Once Rac1 is activated by guanine nucleotide exchange factors (GEFs) at the leading edge, the activated form (GTP-bound Rac1) recruits a complex containing its downstream effector Wiskott–Aldrich Syndrome protein family verprolin homologous to the plasma membrane, leading in turn to activation of the actin-related protein 2/3 (Arp2/3) complex[10,11]. Activated Arp2/3 complex functions as an efficient nucleator[10,11] to organize the branched actin-filament network involved in formation of lamellipodia, a critical step in cell migration.

Some drugs in clinical use have the potential to indirectly activate AMPK. These compounds have been convincingly shown to prevent atherosclerosis, vascular remodelling, and tumour invasion and metastasis[12–17], processes in which dysregulated cell migration contributes to the development and progression of diseases. Accordingly, the clinically beneficial effects of chemical AMPK activators can be partially attributed to inhibition of cell migration via augmentation of AMPK activity. However, the mechanisms by which augmented AMPK activity inhibits cell migration remain largely unknown.

In this study, we identified PDZ and LIM domain 5 (Pdlim5)[18] as a novel substrate of AMPK; Pdlim5 is directly phosphorylated by AMPK at Ser177. This phosphorylation results in displacement of Rho GEF 6 (Arhgef6), a Rac1/Cdc42-specific GEF and also known as p21-activated kinase-interacting exchange factor-αPIX, from the leading edge of the cell by disrupting the association between Pdlim5 and Arhgef6. Displacement of Arhgef6 suppresses Rac1 activity and the disappearance of Arp2/3 complex from the cell periphery, leading to defects in lamellipodia formation and inhibition of directional cell migration. We propose that Pdlim5 is the main signalling molecule that regulates cell migration in the context of augmented AMPK activity.

Results

Pdlim5 is phosphorylated at Ser177 by AMPK. Our group has worked on AMPK for many years. To estimate the AMPK activity level *in vivo*, we often monitor phospho-acetyl-CoA carboxylase (pACC), a well-known substrate of AMPK whose level generally reflects the AMPK activity[4]. When we treated C2C12 cells with AMPK activators such as 5-aminoimidazole-4-carboxyamide ribonucleoside (AICAR), A-769662 and 2-deoxy-D-glucose (2-DG), we serendipitously observed reproducible and specific induction of a protein with an apparent molecular mass of 64 kDa (p64) that cross-reacted with a commercially available antibody against pACC (Fig. 1a and Supplementary Fig. 1a,b, respectively). Three-step column chromatography followed by mass-spectrometric analysis revealed that p64 was likely to be Pdlim5 (ref. 19; Fig. 1b,c). To confirm this, we generated three polyclonal antibodies against mouse Pdlim5 (Supplementary Fig. 1c) and designed two different small interfering RNAs (siRNAs) against the *Pdlim5* messenger RNA (Supplementary Fig. 1d). When we treated C2C12 cells with siPdlim5, the p64 band disappeared (Fig. 1d). Therefore, we concluded that p64 is indeed Pdlim5. Furthermore, as the p64 band, probably representing a phosphorylated form of Pdlim5, was detected exclusively after AMPK activation, we speculated that Pdlim5 is a substrate of AMPK. Pdlim5, also known as Enigma homolog protein, is an α-actinin-binding protein that possesses a PDZ domain at its amino terminus and three LIM motifs at its carboxy terminus[19]. Pdlim5 anchors to the actin cytoskeleton via its PDZ domain and recruits LIM-associated proteins to actin filaments[20]. To narrow down the location of the phosphorylation site, we transfected wild-type (WT) Pdlim5 or deletion mutants (Supplementary Fig. 2a) into HEK293T cells, and then treated the transfectants with AICAR. A mutant truncated after N184 cross-reacted with the pACC antibody following AMPK activation (Supplementary Fig. 2b), whereas a mutant truncated after N160 did not, indicating that the phosphorylation site resides within the N-terminal segment of Pdlim5 between Ala161 and Asn184.

Next, we introduced Ser-to-Ala or Thr-to-Ala point mutations into this putative phosphorylation segment (Fig. 2a). Both the S175A and S177A mutants lost cross-reactivity with pACC antibody (Fig. 2a). Next, we performed *in vitro* phosphorylation assays on recombinant FLAG-tagged Pdlim5 (WT, S175A and S177A). The results revealed that incorporation of [γ-^{32}P]ATP into Pdlim5 was inhibited only in the S177A mutant, indicating that Ser177 is the unique phosphorylation site of Pdlim5 (Fig. 2b). We confirmed direct phosphorylation of Pdlim5 at Ser177 by AMPK by *in vitro* phosphorylation assay using recombinant glutathione *S*-transferase (GST)-fused Pdlim5 (WT or S177A) expressed in *Escherichia coli* (Supplementary Fig. 2c,d), and subsequently by using an antibody we generated (Supplementary Fig. 2e) against Ser177-phosphorylated Pdlim5 (Ab-pS177) (Fig. 2c). The amino-acid sequence surrounding Ser177 matches the consensus sequence for AMPK phosphorylation sites (Supplementary Fig. 2f) and also exhibits a high similarity with the phosphorylation site of ACC (Supplementary Fig. 2f). Furthermore, Ser177, but not Ser175, is highly conserved only in mammals (Supplementary Fig. 3). Next, we confirmed that endogenous Pdlim5 is phosphorylated at Ser177 on AMPK activation *in vivo* in vascular smooth muscle cells (vSMCs) (Fig. 2d and Supplementary Fig. 4). Finally, we investigated whether Pdlim5 is phosphorylated in response to an acute physical stimulus. Hypoxia (1% O_2 for 2 h) activated AMPK and induced Ser177-phosphorylation of Pdlim5 (Fig. 2e). Together, these data indicated that augmented AMPK activity induces Ser177 phosphorylation of Pdlim5 both *in vitro* and *in vivo*.

Ser177 phosphorylation of Pdlim5 inhibits cell migration. To accurately assess the functions of Ser177 phosphorylation of Pdlim5 by AMPK, it is essential to use a system that eliminates any effects associated with AMPK activation other than Ser177 phosphorylation. For this purpose, we established the knockdown-rescue (KDR) system in vSMCs by depleting endogenous Pdlim5 and simultaneously expressing siPDLIM-resistant enhanced green fluorescent protein (EGFP)-tagged Pdlim5 (Fig. 3a). For this purpose, we treated cells with siRNA oligonucleotides targeting the 3′-untranslated region mRNA of mouse Pdlim5 (siPdlim5-2) and infected them with adenovirus encoding EGFP-WT-, EGFP-S177A- or EGFP-S177D-Pdlim5, yielding cells we designated KDR/WT-, KDR/S177A- or KDR/

© 2015 Macmillan Publishers Limited. All rights reserved.

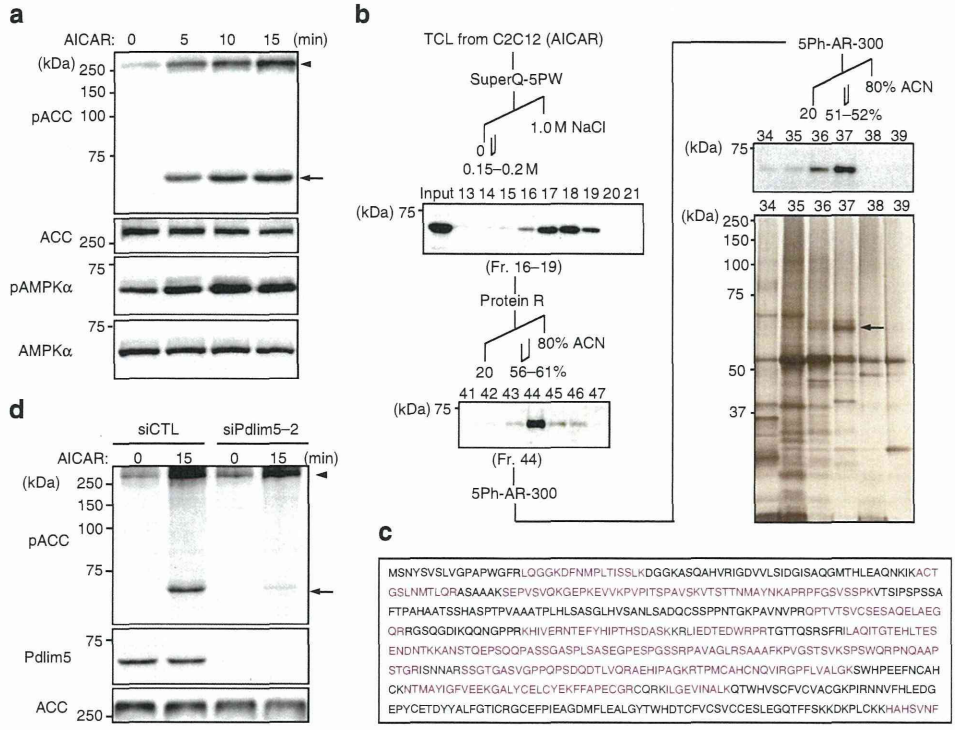

Figure 1 | Pdlim5 is a substrate of AMPK. (**a**) C2C12 cells were stimulated with AICAR (2 mM) 12 h after serum starvation. Total cell lysates (TCLs) were harvested 0, 5, 10 and 15 min after stimulation and subjected to immunoblotting with anti-pACC antibody. In addition to the predicted band for pACC (arrowhead), a cross-reacting band, p64 (arrow), was detected in a time-dependent manner after AICAR treatment. (**b**) A schematic representation of the purification and identification of p64. TCLs from C2C12 cells treated with AICAR were subjected to three-step column chromatography (superQ-5PW, protein R and 5Ph-AR-300). p64 was detected using the anti-pACC antibody in each step. Images were obtained by immunoblotting and silver staining. The identified band (arrow in silver-stained gel), fractionated by reverse-phase HPLC (5Ph-AR-300), was excised and analysed by mass spectrometry. (**c**) Amino acid sequence of Pdlim5. Sequence analysis by MALDI-Qq-TOF MS/MS revealed the target protein to be Pdlim5. Matching amino acids are shown in magenta letters. (**d**) C2C12 cells treated with siRNA (siCTL or siPdlim5-2) were stimulated with AICAR and TCLs were subjected to immunoblotting with pACC and Pdlim5 antibodies (Ab229-2). Arrowhead and arrow denote pACC and p64, respectively.

S177D-Pdlim5, respectively. This KDR system successfully replaced endogenous Pdlim5 with EGFP-Pdlim5 at physiological expression levels in vSMCs (Fig. 3a). Exogenously expressed EGFP-Pdlim5 co-localized with α-actinin and F-actin structures (Fig. 3b), a pattern similar to that of endogenous Pdlim5 (Supplementary Fig. 5), although EGFP-Pdlim5 appeared in the cytoplasm at much higher levels than the endogenous protein. Importantly, EGFP-WT-Pdlim5 was phosphorylated by AMPK in the same manner as endogenous Pdlim5, whereas EGFP-S177A-Pdlim5, an unphosphorylatable mutant, was not phosphorylated (Fig. 3c). EGFP-S177D-Pdlim5, a phosphomimetic mutant, was recognized by the Ab-pS177 antibody even in the absence of AICAR stimulation (Fig. 3c). This result indicates that phosphorylated WT-Pdlim5 and the S177D-Pdlim5 mutant are structurally similar. Thus, even in the absence of AMPK activators, exogenously expressed EGFP-S177D-Pdlim5 behaved similar to endogenous Pdlim5 phosphorylated by AMPK. It is particularly noteworthy that the KDR system can exclude any effects associated with AMPK activation other than Ser177 phosphorylation of Pdlim5.

AMPK activation inhibits cell migration; to investigate whether this effect is mediated by Pdlim5 phosphorylation at Ser177, we performed a scratch assay using the KDR/vSMC system in the absence of AMPK activators. KDR/S177D-Pdlim5 cells exhibited a marked delay in scratch closure relative to both KDR/WT- and KDR/S177A-Pdlim5 cells (Fig. 3d,e and Supplementary Movie 1). By tracking the movement of individual cells, we could calculate the path length (L) and displacement (D) of individual cells (Fig. 3f). KDR/S177D-Pdlim5 cells exhibited a lower migration speed (defined as L/total trajectory time) and less directionality (defined as D/L) than KDR/WT- and KDR/S177A-Pdlim5 cells (Fig. 3g,h). Next, we performed a scratch assay in the presence of AMPK activator (Supplementary Fig. 6). Compared with KDR/WT- and KDR/S177D-Pdlim5 cells, the degree of cell migratory inhibition was lower in KDR/S177A-Pdlim5 cells (Supplementary Fig. 6). Furthermore, we examined single-cell migration in the absence of AMPK activators. Consistent with the results of the scratch assay, KDR/S177D-Pdlim5 cells exhibited impaired cell migration (Supplementary Fig. 7a,b and Supplementary Movie 2).

Next, we examined the AMPK specificity of the phenotypes observed in KDR cells using AMPKα1$^{-/-}$α2$^{-/-}$ mouse embryonic fibroblasts (AMPKα-null MEFs). First, we confirmed that Pdlim5 phosphorylation by AMPK activators was completely blocked in AMPKα-null MEFs (Fig. 4a and Supplementary Fig. 8). Moreover, a scratch assay confirmed that AMPK activator-induced cell migratory inhibition was abolished in AMPKα-null MEFs (Fig. 4b–d and Supplementary Movie 3). For further confirmation, we constructed a Pdlim5 knockout vSMC (Pdlim5$^{-/-}$ vSMC) line by genome editing, using the CRISPR/Cas9 system (Supplementary Fig. 9), and established a knockout and rescue cell system by expressing EGFP-Pdlim5 (WT, S177A or S177D) at physiological level by adenovirus transduction of knockout cells (Supplementary Fig. 10a). When the knockout and rescue cells were subjected to a cell migration assay (Supplementary Fig. 10b–d), the results were consistent with

© 2015 Macmillan Publishers Limited. All rights reserved.

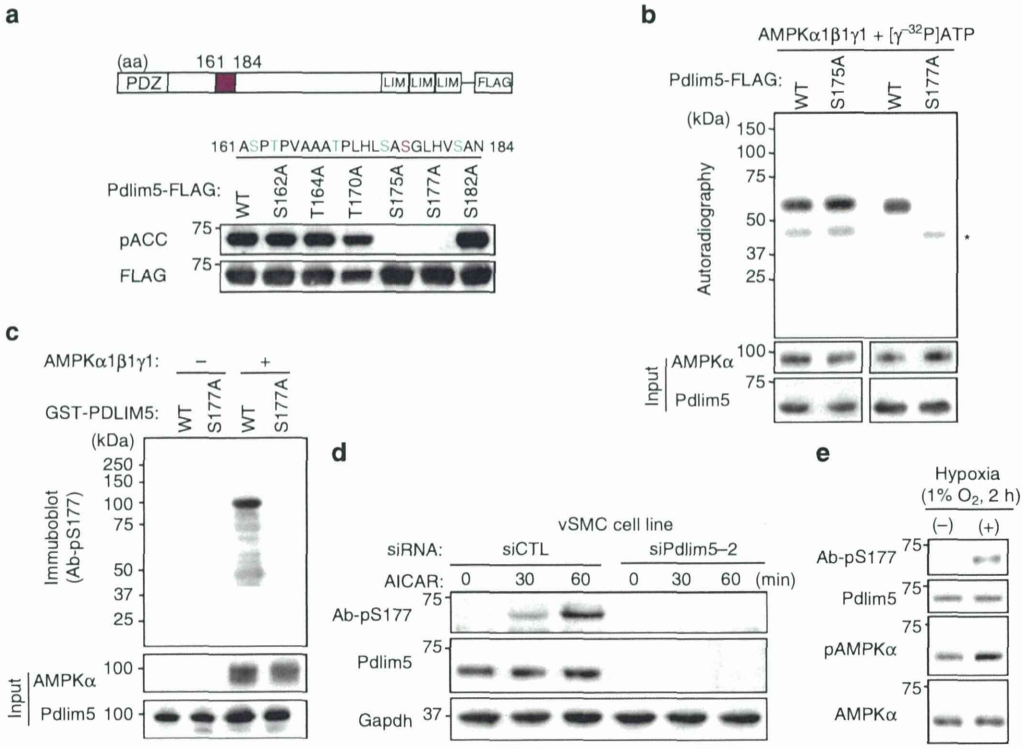

Figure 2 | Pdlim5 is directly phosphorylated at Ser177 by AMPK. (**a**) Diagrams of point-mutated Pdlim5. HEK293T cells were transiently expressed with each point-mutant of cFLAG-tagged Pdlim5 and treated with AICAR (2 mM) for 15 min. Proteins purified on anti-FLAG M2 agarose were subjected to immunoblotting with anti-pACC or anti-FLAG antibody. (**b**) *In vitro* assay for AMPK phosphorylation. Recombinant cFLAG-tagged Pdlim5 (WT, S175A or S177A) from HEK293T cells was incubated with baculovirus-expressed recombinant AMPK in the presence of [γ-^{32}P]ATP and then subjected to autoradiography. Asterisk denotes bands of α-subunit of recombinant AMPK. (**c**) *In vitro* phosphorylation assay by AMPK. Recombinant GST-tagged Pdlim5 proteins (WT and S177A) were incubated with or without recombinant AMPK and then subjected to immunoblotting with Ab-pS177. (**d**) vSMCs transfected either with siCTL or siPdlim5-2 were treated with AICAR (2 mM) for the indicated times, and TCLs were subjected to immunoblotting with Ab-pS177. (**e**) vSMCs were exposed to physiological hypoxia (1% O_2 for 2 h). TCLs were subjected to immunoblotting with the indicated antibodies.

those obtained with the KDR cells. Together, these results indicated that Ser177 phosphorylation of Pdlim5 by AMPK inhibits cell migration.

Ser177 phosphorylation altered actin architectures. To elucidate the mechanism by which Ser177 phosphorylation of Pdlim5 inhibits cell migration, we monitored morphological changes in KDR cells. In all three types of KDR cells, EGFP-Pdlim5 protein co-localized with F-actin at the cell periphery and on stress fibres (Fig. 5a), indicating that co-localization of Pdlim5 with actin was not influenced by the phosphorylation state of Ser177. However, KDR/WT- and KDR/S177A-Pdlim5 cells displayed smooth lamellipodia-like edges, whereas KDR/S177D-Pdlim5 cells exhibited attenuated lamellipodia formation and jagged edges with excessive filopodia-like protrusions and ventral stress fibres (Fig. 5a and Supplementary Fig. 11a). In addition, both KDR/WT- and KDR/S177A-Pdlim5 cells contained small and scattered spots of focal adhesions at the junction between the lamellipodia and lamella; by contrast, in KDR/S177D-Pdlim5 cells, focal adhesions were displaced to the edge of the cell and significantly enlarged in size (Fig. 5a and Supplementary Fig. 11b). To determine whether the morphological changes observed in KDR/S177D-Pdlim5 cells were related to Ser177 phosphorylation of Pdlim5, we performed time-lapse imaging before and after treatment with AMPK activator (Fig. 5b,c). In KDR/WT-Pdlim5 cells, but not in KDR/S177A-Pdlim5 cells, AMPK activation induced defective lamellipodia formation and promoted expansion of the EGFP signals from the side opposite the lamellae towards the cell centre (Fig. 5b,c and Supplementary Movie 4), a pattern resembling the growth of dorsal stress fibres. This morphological change was similar to that observed in KDR/S177D-Pdlim5 cells. Furthermore, AMPK activation induced defective lamellipodia and enhanced stress fibre formation in WT-MEFs, but not AMPKα-null MEFs (Fig. 4e). These findings suggested that Ser177 phosphorylation of Pdlim5 by augmented AMPK activity induced attenuation of lamellipodia and promoted formation of stress fibres from the cell periphery. Furthermore, these observations suggested that morphological changes of the actin architecture were initiated near the cell periphery.

Ser177 phosphorylation altered Arp2/3 complex localization. Accordingly, we focused on the Arp2/3 complex, because it is one of the major actin nucleators at the cell periphery and plays a key role in lamellipodia formation[10]. Expression levels of Arp2/3 complex were comparable among the various types of KDR cells (Supplementary Fig. 12a). However, the intracellular localization of Arp2/3 complex was markedly altered in both spreading and polarized cells (Fig. 6). In spreading cells, KDR/WT-Pdlim5 cells exhibited highly uniform lamellipodia throughout the cell edge, where Arp3 predominantly localized (Fig. 6a). By contrast, KDR/S177D-Pdlim5 cells exhibited filopodia-like protrusions instead of lamellipodia, and localization of Arp3 shifted from the cell edge to a cytoplasmic distribution (Fig. 6a). A similar pattern was observed in polarized cell: Arp3 localized in actin-rich

© 2015 Macmillan Publishers Limited. All rights reserved.

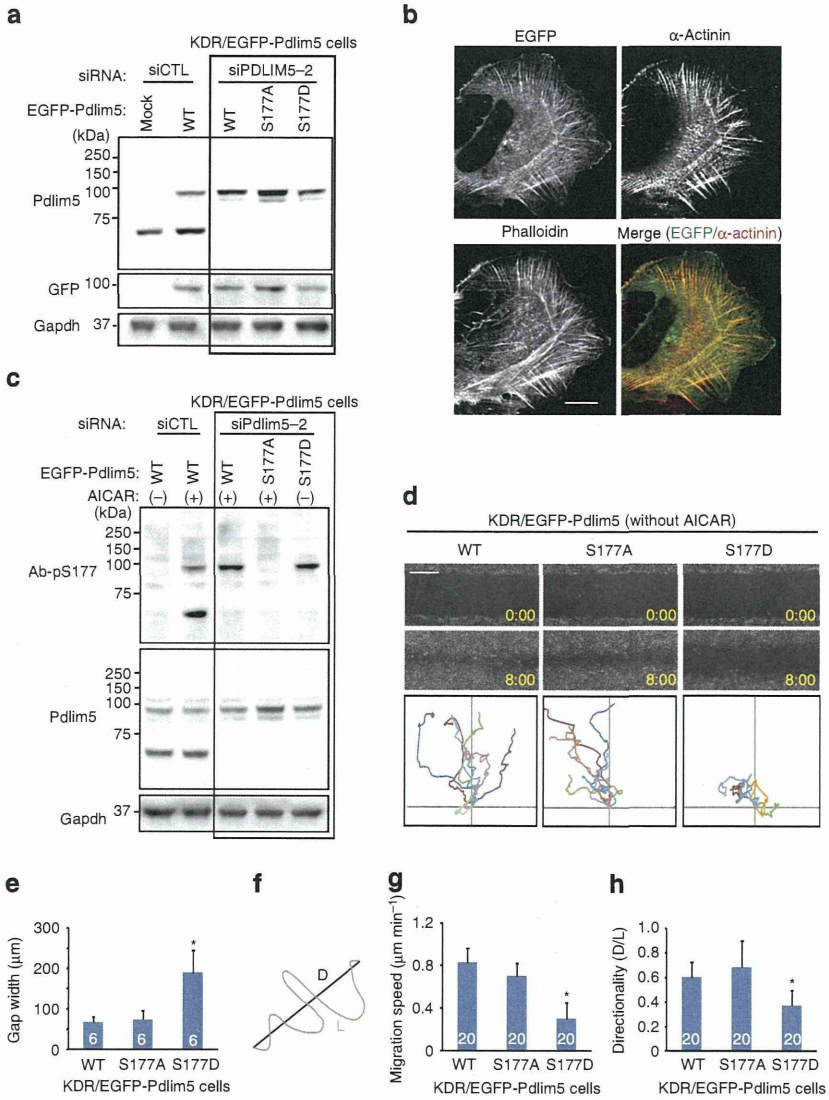

Figure 3 | Ser177 phosphorylation of Pdlim5 by AMPK inhibited directional migration of vSMCs. (**a**) Establishment of the KDR system for Pdlim5 in vSMCs. vSMCs were transfected with either siCTL or siPdlim5-2. siPdlim5-2-resistant EGFP-Pdlim5 (WT, S177A or S177D) was added back by adenoviral-mediated gene delivery. TCLs were subjected to immunoblotting. (**b**) GFP and immunostained images of KDR/EGFP-WT-Pdlim5 cells stained with a α-actinin antibody and phalloidin. Scale bar, 10 μm. (**c**) KDR/EGFP-Pdlim5 (WT and S177A) cells were treated with AICAR for 60 min, whereas KDR/EGFP-S177D-Pdlim5 cells were not treated with AICAR. TCLs from each cell were subjected to immunoblotting. (**d**) Scratch assay of KDR/EGFP-Pdlim5 cells. Phase-contrast microscopy images of KDR/Pdlim5 cells (WT, S177A and S177D) before and 8 h after scratching in the absence of AICAR. The bottom row of each panel shows analysis of migration paths over 8 h. The origins of migration of each cell were superimposed at [0, 0]. Scale bar, 0.5 mm. (**e**) Bar graph showing the gap width 8 h after scratching (from **d**). (**f**) Demonstration of path length (L) and displacement (D) for calculation of migration velocity and directionality. (**g**) Bar graph showing migration speed of each cell (from **d**). (**h**) Bar graph showing migration directionality of each cell (from **d**). Numbers in the bars indicate *n*. Data are representative of means ± s.e.m. from three independent experiments. Significance of differences between series of results was assessed using one-way analysis of variance, followed by a *post-hoc* comparison with Dunnett's method for multiple comparisons. $^{*}P<0.01$ compared with WT.

lamellipodia in KDR/WT-Pdlim5 cells, but was distributed diffusely throughout the cytoplasm in KDR/S177D-Pdlim5 cells (Fig. 6b). These findings indicated that Ser177 phosphorylation of Pdlim5 impairs the function of the Arp2/3 complex by altering the localization of the complex from the cell edge to the cytoplasm. Consistent with this, vSMCs defective for Arp2/3 complex due to knockdown of the Arpc2 subunit exhibited a phenotype very similar to that of DR/S177D-Pdlim5 cells (Supplementary Fig. 12b,c). On the other hand, mammalian diaphanous (mDia), another actin nucleator, persisted at the leading edge of the cells (Supplementary Fig. 13).

Ser177 phosphorylation of Pdlim5 decreased Rac1 activity. Next, we measured the activities of Rac1, an upstream regulator of the Arp2/3 complex that is required for lamellipodia formation[8,9]. GTP-bound active Rac1 was significantly reduced in KDR/S177D-Pdlim5 cells relative to KDR/WT- and KDR/S177A-Pdlim5 cells (Fig. 7a). Furthermore, we carried out imaging of Rac1 activity in living cells, using vSMCs stably expressing the Raichu-Rac1 probe (vSMC-R_{Rac1} cells), which is based on the principle of fluorescence resonance energy transfer (FRET) biosensors[21]. We established the KDR system in vSMC-R_{Rac1} cells, as described above, except that siPDLIM-resistant Pdlim5

© 2015 Macmillan Publishers Limited. All rights reserved.

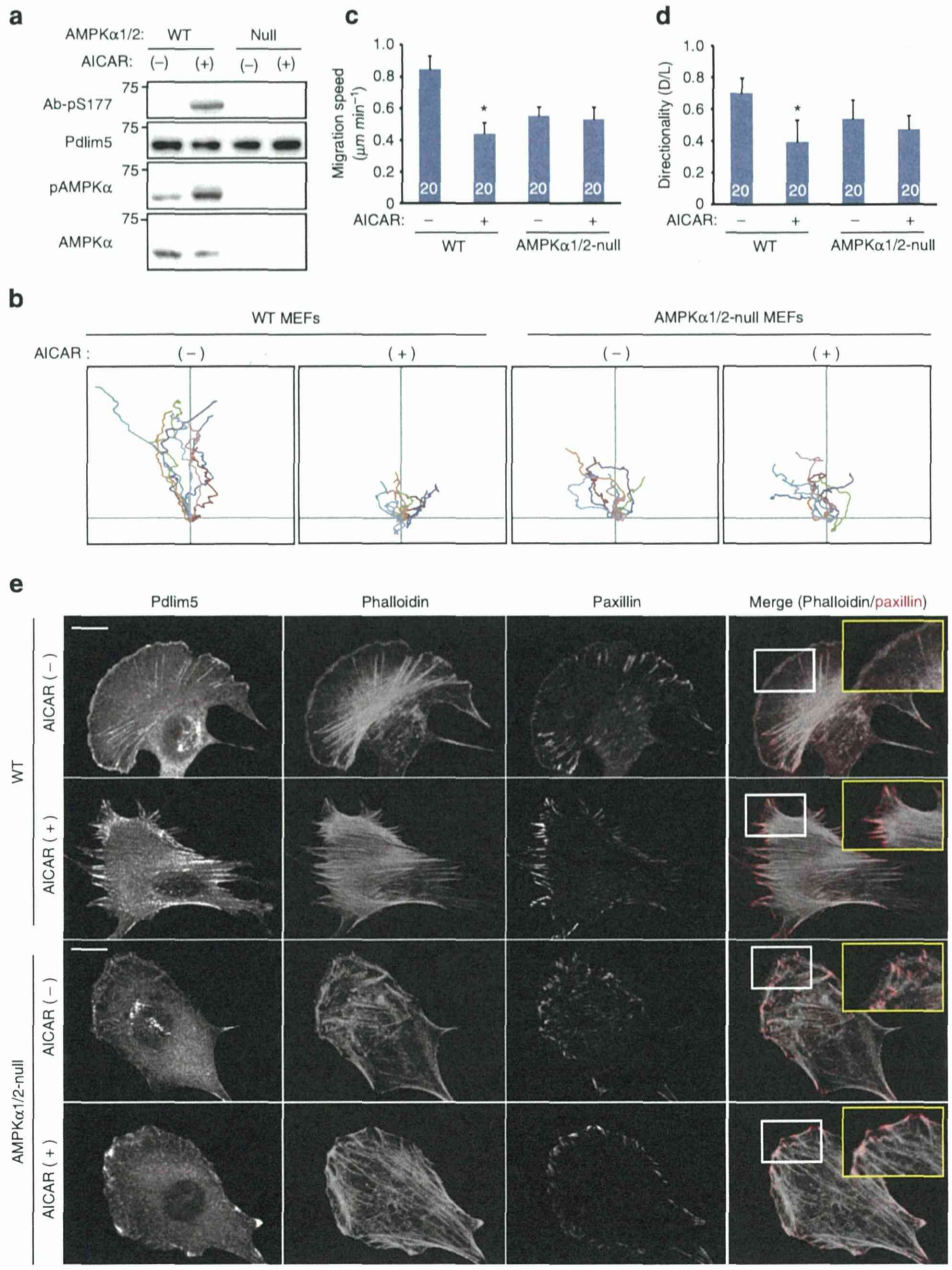

Figure 4 | Pdlim5 phosphorylation was blocked in AMPKα1/2-null MEFs. (**a**) WT or AMPKα1/2-null MEFs were stimulated with AICAR (1 mM) for 15 min. TCLs were subjected to immunoblotting with indicated antibodies. (**b**) Phase-contrast images of WT-MEFs and AMPKα1/2-null MEFs were collected during the scratch assay in the presence or absence of AICAR (1 mM). Each panel shows analysis of migration paths over 8 h. The origins of migration of each cell were superimposed at [0, 0]. (**c**) Bar graph showing the migrating speed of each cell (from **b**). (**d**) Bar graph showing migration directionality of each cell (from **b**). Numbers in the bars indicate *n*. Data are representative of means ± s.e.m. from three independent experiments. Significance of differences between series of results was assessed using one-way analysis of variance, followed by a *post-hoc* comparison with Dunnett's method for multiple comparisons. $^{*}P<0.01$ compared with WT without AICAR treatment. (**e**) Immunostained images of WT-MEFs and AMPKα1/2-null MEFs in the presence or absence of AICAR (1 mM). These cells were stained with a Pdlim5 antibody, phalloidin and anti-paxillin antibody. Magnified images outlined by yellow squares show the areas outlined by white squares. Scale bar, 10 μm.

was co-expressed with mCherry instead of being tagged with EGFP (Raichu-Rac1/KDR/Pdlim5-T2A-mCherry) (Fig. 7d). Rac1 activity was lower in cells expressing S177D-Pdlim5 than in those expressing WT-Pdlim5 or S177A-Pdlim5, especially in the cell periphery (Fig. 7e and Supplementary Fig. 14). Thus, these findings indicated that Rac1 activity was suppressed in cells expressing S177D-Pdlim5, especially in the cell periphery, resulting in dislocation of the Arp2/3 complex. On the other hand, we observed no changes in RhoA or Cdc42 activity (Fig. 7b,c and Supplementary Fig. 15).

Pdlim5 phosphorylation altered the interaction with Arhgef6. To investigate the molecular mechanism by which S177D-Pdlim5 suppresses Rac1 activity, we performed GST pull-down assays followed by high-sensitivity shotgun liquid chromatography–mass

© 2015 Macmillan Publishers Limited. All rights reserved.

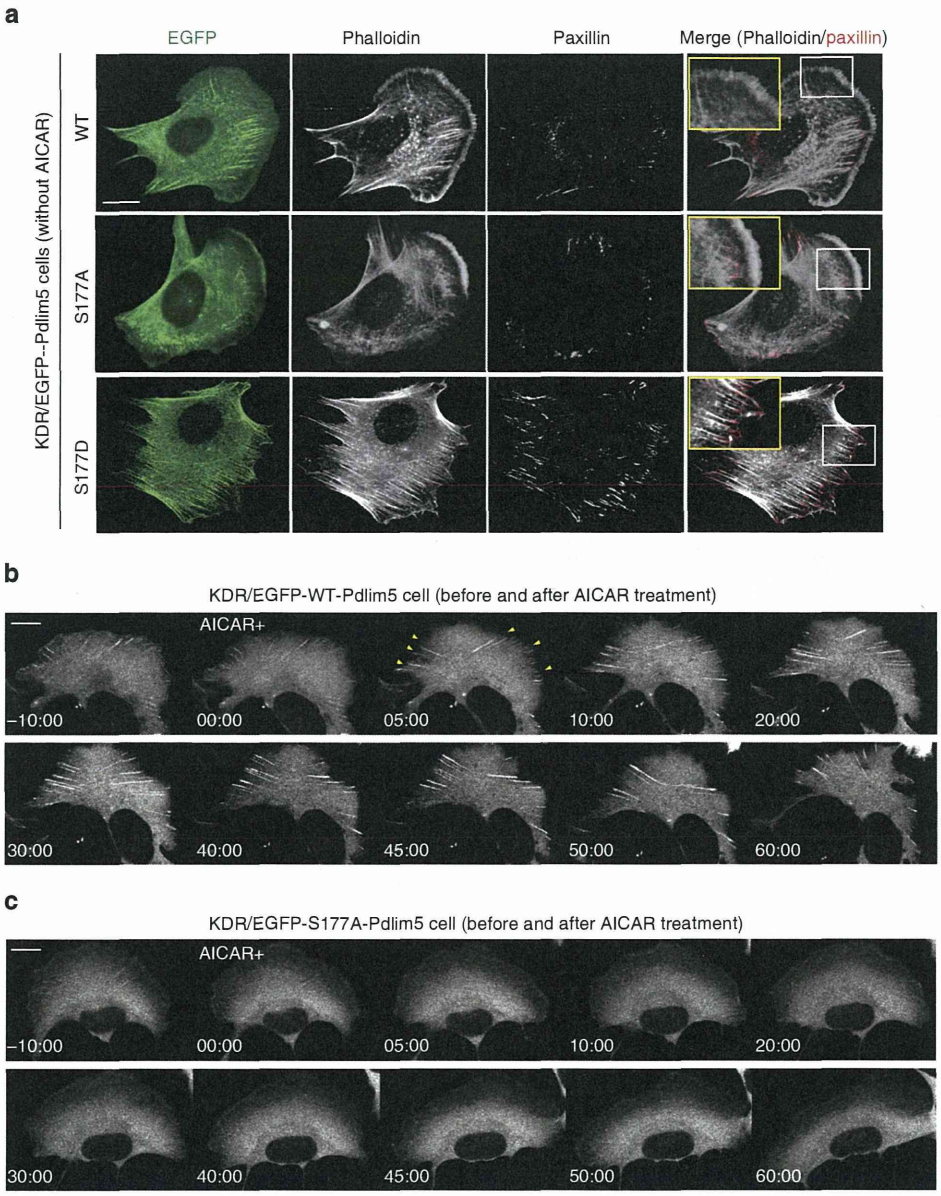

Figure 5 | Ser177 phosphorylation of Pdlim5 causes reorganization of lamellipodia, stress fibres and focal adhesions. (**a**) GFP images (left) and immunostained images of KDR/EGFP-Pdlim5 cells (WT, S177A and S177D). Cells were stained with phalloidin and anti-paxillin antibody, to visualize actin microfilaments and focal adhesions, respectively. Magnified images outlined by yellow squares show the area outlined by the white squares. Scale bar, 10 μm. (**b**,**c**) Sequential GFP images of KDR/EGFP-WT-Pdlim5 (**b**) or KDR/EGFP-S177A-Pdlim5 (**c**) cells before and after AICAR stimulation (2 mM). Yellow arrowheads represent dorsal stress fibres growing from the opposite side after AICAR treatment of KDR/EGFP-WT-Pdlim5 cells. Scale bar, 10 μm.

spectrometry, using total cell lysates from U937 cells. Among a total of 1,225 proteins detected, several RhoGEFs were more prominently associated with GST-WT-Pdlim5 than with GST-S177D-Pdlim5 (Supplementary Table 1). Among them, we focused on Arhgef6, because it exclusively associated with WT-Pdlim5 (Fig. 8a) and can activate Rac1 at the leading edge of migrating cells[22,23]. Both the biochemical dissociation of Arhgef6 and S177D-Pdlim5, and the intracellular co-localization of Arhgef6 with Pdlim5 at the cell periphery were disrupted in KDR/S177D-Pdlim5 cells (Fig. 8b). These findings suggested that Ser177 phosphorylation of Pdlim5 disrupted the recruitment of Arhgef6 at the cell's leading edge, potentially suppressing Rac1 activity. Next, we compared the effect of Arhgef6 knockdown on cell migration and morphology with that of Ser177 phosphorylation of Pdlim5 (Fig. 8c and Supplementary Fig. 16). The similarity was only partial: Arhgef6-knockdown vSMCs exhibited a disturbed migration relative to control vSMCs (Supplementary Fig. 16b–d) and defective lamellipodia (Fig. 8c), but not elevated formation of stress fibres (Fig. 8c).

Pdlim5 recruits AMPK onto actin filaments. To investigate how AMPK signalling is transmitted to peripheral actin filaments, we examined the physical link between actin filaments, Pdlim5 and AMPK. Immunoprecipitation/immunoblotting of HEK293T cells co-transfected with V5-tagged AMPKα and FLAG-tagged Pdlim5 (WT, ΔPDZ or ΔLIM) demonstrated that AMPK bound to Pdlim5 through the LIM domain (Fig. 9a). Next, we performed an F-actin-binding assay, in which F-actin and its binding proteins are found in the pellet fraction, to determine whether Pdlim5

© 2015 Macmillan Publishers Limited. All rights reserved.

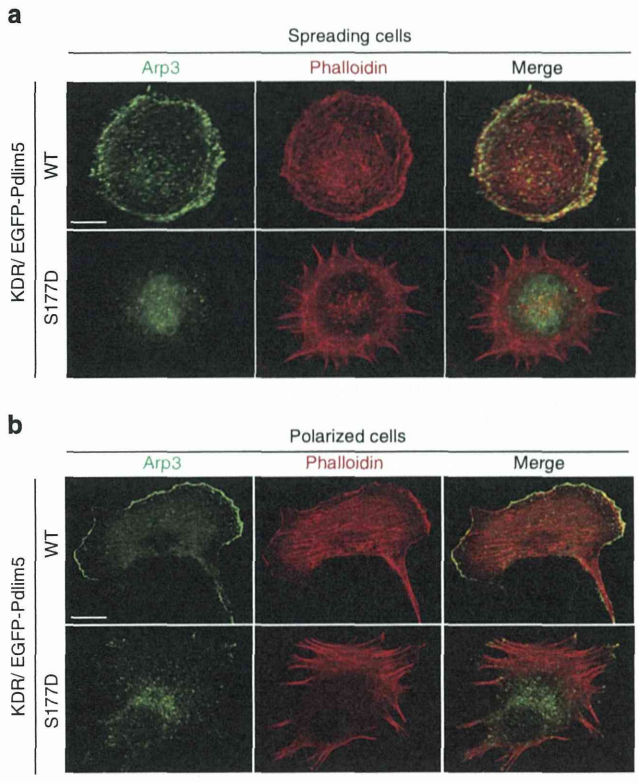

Figure 6 | Ser177 phosphorylation of Pdlim5 leads to altered Arp2/3 complex localization. (**a**,**b**) Immunostaining of spreading (**a**) or polarized (**b**) KDR/EGFP-Pdlim5 cells. Cells were fixed and stained with an Arp3 antibody and phalloidin. Scale bars, 10 μm.

promotes the recruitment of AMPK onto actin filaments. In the absence of Pdlim5, AMPK was found exclusively in the supernatant (Fig. 9b). However, in the presence of Pdlim5, AMPK shifted from the supernatant to the pellets and this shift was greatly stimulated by the presence of α-actinin (Fig. 9b). These findings indicate that Pdlim5 binds AMPK directly and promotes the recruitment of AMPK onto F-actin, a process mediated by α-actinin.

Discussion

The results described here reveal the mechanism by which augmented AMPK activity inhibits cell migration. In this study, we serendipitously identified Pdlim5 as a novel substrate of AMPK. On augmentation of AMPK activity, Pdlim5 was phosphorylated at Ser177, disrupting its association with Arhgef6 at the cell periphery and suppressing Rac1 activity at the leading edge of cell. Suppression of Rac1 activity dislocated the Arp2/3 complex from the leading edge, resulting in attenuation of lamellipodia formation and inhibition of cell migration.

We previously established a unique screening method using two-step column chromatography combined with an *in vitro* kinase reaction. Using this method, we identified CLIP-170 as a novel AMPK substrate[4]. In this study, we identified Pdlim5 as another substrate of AMPK by probing cells with a pACC antibody after AMPK activation. The amino-acid sequence surrounding Ser177 of Pdlim5 is very similar to a sequence in ACC, which may explain why we were able to discover this new AMPK substrate using a pACC antibody. Importantly, Pdlim5 is not phosphorylated at all before stimulation with AMPK activators, whereas other AMPK substrates such as ACC and CLIP-170 (ref. 4) are already phosphorylated to some extent even before stimulation. These findings suggest that Pdlim5 is phosphorylated only under stressed conditions in which AMPK activity is augmented. Accordingly, we conclude that the functional impact of Pdlim5 phosphorylation by AMPK is exerted only under cellular conditions associated with augmented AMPK activity. Thus, Pdlim5 phosphorylation might cause different biological effects than phosphorylation of other AMPK substrates.

In mouse, the double knockout of AMPKα1α2 (AMPKα1$^{-/-}$α2$^{-/-}$) is early embryonic lethal[24], but AMPKα-null MEFs are viable[25]. AMPK-null cells exhibit a metabolic shift towards aerobic glycolysis[26], as well as abnormalities in cell polarity and cellular structures[2]. Pharmacological inhibition of AMPK also perturbs cell polarity and migration[4]. Thus, it is reasonable to conclude that AMPK activity affects directional cell migration by regulating cell polarity. However, as AMPK has many substrates other than Pdlim5, it is still difficult to infer the role of Pdlim5 phosphorylation from the lethal phenotype of the AMPKα1$^{-/-}$α2$^{-/-}$ mouse. On the other hand, two studies have reported different phenotypes of Pdlim5 homozygous knockout mice: dilated cardiomyopathy[27] and embryonic lethality probably due to embryonic heart/circulation failure[28]. Pdlim5 associates with the actin cytoskeleton and promotes the assembly of protein complexes by acting as a scaffold protein, and thus recruit proteins that modulate cell architecture, actin dynamics and signal transduction[19] to the actin filaments. Therefore, both phenotypes of Pdlim5 homozygous knockout mice may be attributed to the loss of organized cytoskeletal structures due to progressive loss of protein complex components. Similarly, we postulate that Pdlim5 and its phosphorylation play an important role in regulation of cell morphology and migration, although no previous reports have described the cell migratory behaviour of Pdlim5-knockout cells.

In this study, we focused on determining how AMPK-induced Ser177 phosphorylation of Pdlim5 inhibits cell migration. We found that Pdlim5 localized on actin-filament structures such as stress fibres and focal adhesions, as well as at the cell cortex (including lamellipodia), and that Ser177 phosphorylation itself did not influence Pdlim5 localization. However, the phosphomimetic mutant S177D-Pdlim5 caused characteristic morphological changes such as defective lamellipodia, enhanced ventral stress fibres and displacement of focal adhesions to the cell edge. These specific morphological changes at the cell edge were also observed on pharmacological activation of endogenous AMPK. Thus, the major initial morphological changes resulting from Ser177 phosphorylation of Pdlim5 seemed to arise from the cell cortex. Arhgef6 belongs to the Dbl family of GEFs, defined by the presence of tandem Dbl homology and Pleckstrin homology domains, and functions as a Rac-specific GEF at the cell periphery[22,23,29]. Arhgef6 is recruited to a signalling complex consisting of integrin-linked kinase, particularly interesting cysteine–histidine-rich protein and parvin (IPP complex) by binding to parvin[30,31] (Fig. 10), which plays an important role in cell spreading and motility[32], and may be involved in the Pdlim5 phosphorylation signal mediated by Arhgef6. The IPP complex assembles at small focal complexes at the tips of lamellipodia of migrating cells and then interacts with the cytoplasmic tails of β-integrin molecules to connect them to the actin cytoskeleton[32]. Thus, Arhgef6 activates Rac1 and reorganizes the actin cytoskeleton around the focal complex of lamellipodia, which is necessary for cell spreading and migration[29]. Moreover, α-actinin also binds to parvin directly[33] and is involved in the IPP complex[31]. As Pdlim5 binds to α-actinin directly[34], it is likely to be that Pdlim5 is recruited to the IPP complex in close proximity to Arhgef6 via binding to α-actinin. It is particularly noteworthy

© 2015 Macmillan Publishers Limited. All rights reserved.

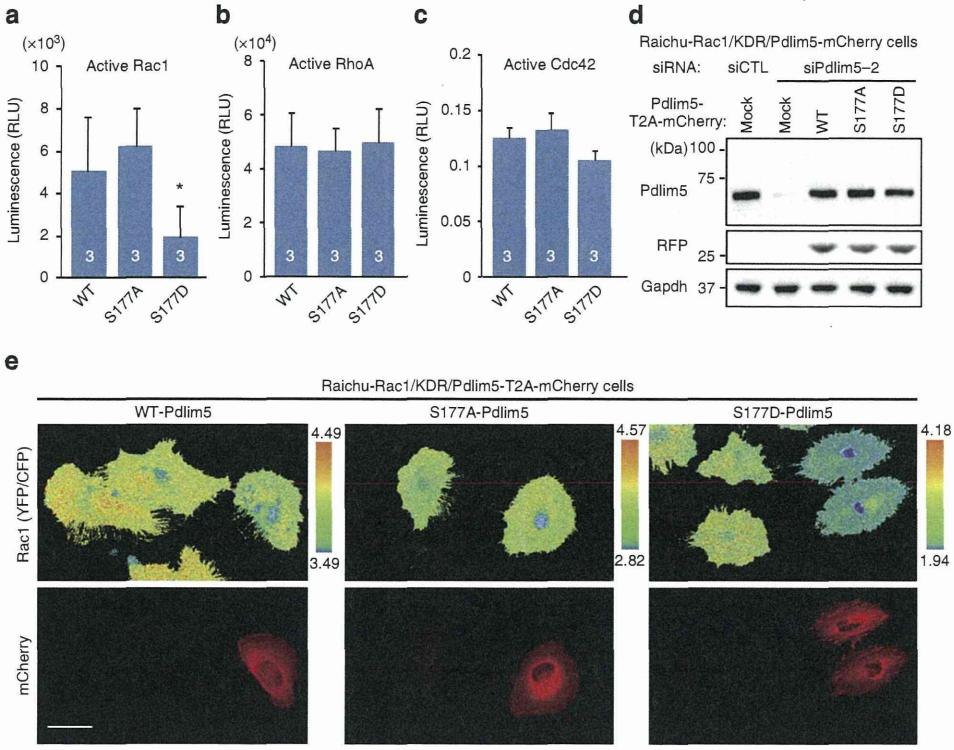

Figure 7 | Ser177 phosphorylation of Pdlim5 suppressed Rac1 activity. (**a**–**c**) Activities of Rac1 (**a**), RhoA (**b**) and Cdc42 (**c**) in KDR cells were quantitated using G-LISA specific for Rac1, RhoA and Cdc42, respectively. Numbers in the bars indicate *n*. Data are representative of means ± s.e.m. from three independent experiments. Significance of differences between series of results was assessed using one-way analysis of variance, followed by a *post-hoc* comparison with Dunnett's method for multiple comparisons. $^{*}P<0.01$ compared with KDR/EGFP-WT-Pdlim5. (**d**) The KDR system was established in vSMCs stably expressing FRET probes specific for Rac1 (Raichu-Rac1/vSMCs). Raichu-Rac1/vSMCs were transfected with either siCTL or siPdlim5-2. siPdlim5-2-resistant Pdlim5-T2A-mCherry (WT, S177A and S177D) was introduced via adenoviral-mediated gene delivery (Raichu-Rac1/KDR-Pdlim5-T2A-mCherry cells). TCLs were subjected to immunoblotting. (**e**) Imaging of Rac1 activity. Each type of Raichu-Rac1/KDR-Pdlim5-T2A-mCherry cell (WT, S177A and S177D) was imaged for YFP and CFP. FRET efficiencies are shown as YFP/CFP ratio images. Scale bars, 20 μm.

that S177D-Pdlim5 disrupted the physical association between Pdlim5 and displaced Arhgef6 from the cell periphery (Fig. 8). These findings led us to speculate that Arhgef6 is displaced from the IPP complex on Ser177 phosphorylation of Pdlim5 by AMPK, resulting in the suppression of Rac1 activity at the cell's leading edge. Rac1 is predominantly localized at the plasma membrane[35] and GTP-bound active Rac1 at the cell periphery can activate Arp2/3 complex through recruitment of the Wiskott–Aldrich Syndrome protein family verprolin homologous complex[10,11]. Therefore, we expected that the function of Arp2/3 complex would also be suppressed in KDR/S177D-Pdlim5 cells. In fact, the Arp2/3 complex was displaced from the cell periphery and distributed throughout the cytoplasm in KDR/S177D-Pdlim5 cells, consistent with a previous study demonstrating that inhibition of Rac1 activity interferes with intracellular localization of the Arp2/3 complex[36]. Furthermore, the morphological characteristics observed in KDR/S177D-Pdlim5 cells were quite similar to those in cells with a functional defect in the Arp2/3 complex[37–39]. As Arp2/3 complexes play a pivotal role in organizing branched actin filament networks to form lamellipodia[10,11], the attenuation of lamellipodia formation and inhibition of cell migration observed in KDR/S177D-Pdlim5 cells was plausible. Thus, our findings strongly suggest that Ser177 phosphorylation of Pdlim5 by AMPK suppresses Rac1 activity by displacing Afhgef6 from the cell periphery, leading to functional suppression of the Arp2/3 complex. However, as the morphological phenotype of Arhgef6-knockdown cells was not entirely consistent with that of KDR/S177D-Pdlim5 cells, we must consider the idea that mechanisms other than the Arhgef6–Rac1–Arp2/3 complex pathway contribute to the phenotypes resulting from Ser177 phosphorylation of Pdlim5. One possible mechanism involves a relative increase in RhoA activity over Rac1 due to a reduction in Rac1 activity, which may contribute to the phenotype even in the absence of elevated RhoA activity. Consistent with this idea, the relative balance between Rac1 and RhoA activities regulates cell morphology and migratory behaviour[40,41]. Another possibility is that other GEFs or GTPase-activating proteins contribute to the phenotype of KDR/S177D-Pdlim5 cells. Indeed, dedicator of cytokinesis 2 is also a Rac-specific GEF and interacted with WT-Pdlim5 more strongly than with S177D-Pdlim5 (Supplementary Table 1).

Another important question relates to the mechanism underlying excessive formation of stress fibres, observed in both vSMCs treated with AMPK activator and KDR/S177D-Pdlim5 cells. In particular, cells stimulated with AMPK activators exhibited striking elongation of dorsal stress fibres from the cell periphery. This finding was in excellent agreement with a previous report demonstrating that Arp2/3-defective cells exhibited a higher growth rate of dorsal stress fibres[39]. The authors of that report proposed that the elevated growth of dorsal stress fibres may result from the increased concentration of cytoplasmic G-actin caused by the absence of Arp2/3-nucleated barbed ends[10]. In addition, mDia remained localized at the cell periphery in KDR/S177D-Pdlim5 cells, whereas Arp2/3 complex moved from the periphery to the cytosol. mDia is another major actin filament nucleator that nucleates linear actin filament at the cell periphery

© 2015 Macmillan Publishers Limited. All rights reserved.

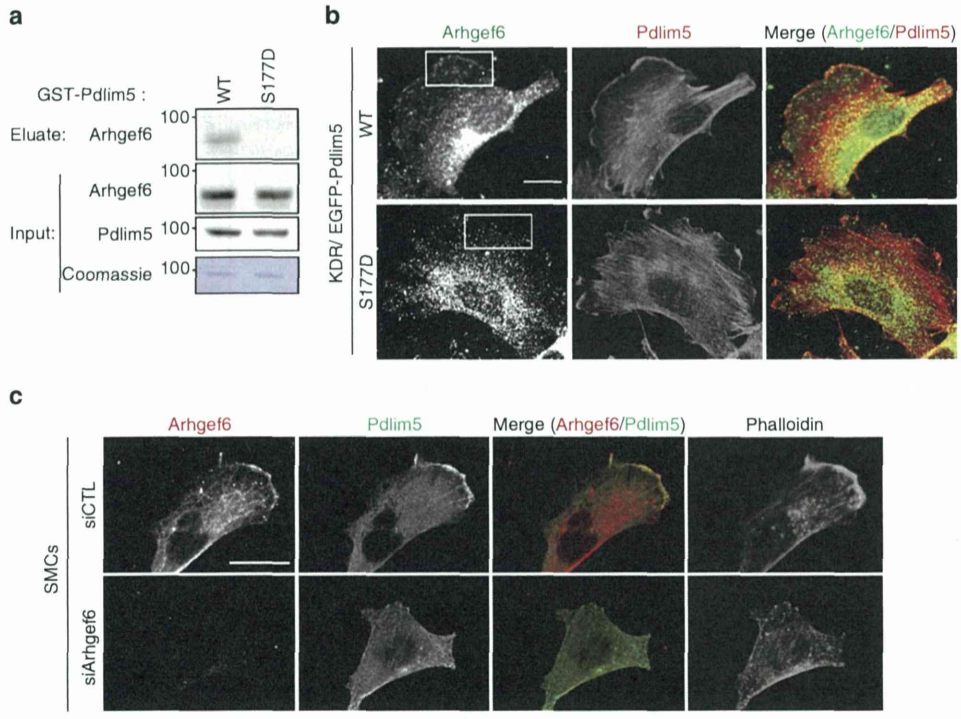

Figure 8 | Ser177 phosphorylation of Pdlim5 disrupts its association with Arhgef6 at the cell periphery. (**a**) Immunoblotting analysis of GST-Pdlim5 pull-down assay. Eluates were subjected to immunoblotting with anti-Arhgef6 antibody. Coomassie staining demonstrates equal loading of GST-Pdlim5 proteins. (**b**) Immunostaining images of Arhgef6 and Pdlim5 from KDR/EGFP-Pdlim5 cells. Boxed area in KDR/EGFP-WT-Pdlim5 cell highlights representative co-localization of Arhgef6 with Pdlim5 at the cell periphery. Scale bars, 10 μm. (**c**) Immunostained images of Arhgef6 knockdown vSMCs stained with anti-Pdlim5 antibody, anti-Arhgef6 antibody and phalloidin. Scale bars, 10 μm.

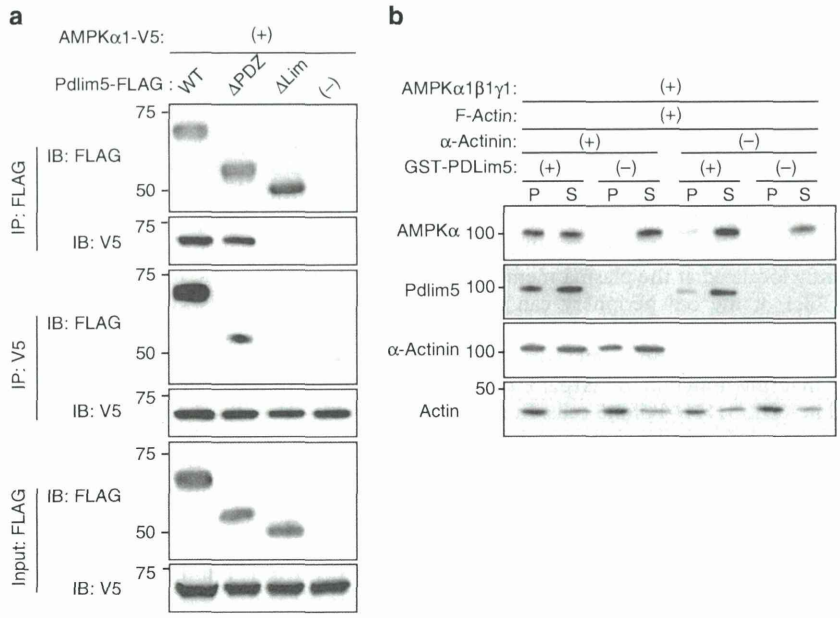

Figure 9 | AMPK is recruited onto F-actin by directly binding the LIM domain of Pdlim5. (**a**) HEK293T cells were co-transfected with V5-tagged AMPKα and FLAG-tagged Pdlim5 (WT, ΔPDZ or ΔLIM domain). TCLs were immunoprecipitated by FLAG or V5 and then immunoblotted with the indicated antibodies. (**b**) F-actin binding assay of AMPK. AMPK was mixed with a fixed amount of F-actin in the presence or absence of α-actinin and GST-Pdlim5, incubated for 1 h at 24 °C and then centrifuged at 150,000 *g* for 1.5 h at 24 °C, to pellet the F-actin polymer and associated proteins. A sample of the pellet (P) and supernatant (S) were analysed by immunoblotting for the indicated antibodies.

and can elongate actin directly proportional to the G-actin monomer concentration[42]. Thus, mDia at the cell periphery under increased G-actin concentration may also contribute to elevated formation of stress fibres and filopodia in KDR/S177D-Pdlim5 cells. Taken together, these data indicate that the morphological and migratory phenotypes observed in cells

© 2015 Macmillan Publishers Limited. All rights reserved.